The Development of Optimized Small Cargo Ship

MARINE 2021

Tomoyo Nakayama[1*], Yoshihiisa Okada[1], Toshie Kajino[1] and Masahiro Tamashima[2]

[1] Nakashima Propeller Co., Ltd., 688-1, Joto-Kitagata, Higashi-ku, Okayama 709-0625, Japan.
Email: t-kaga@nakashima.co.jp, yoshihisa@nakashima.co.jp, t-kajino@nakashima.co.jp,
web: https://www.nakashima.co.jp/

[2] Fluid Techno Co., Ltd., 6F Gibraltar Seimei Bldg 1-7, Tokiwa-cho, Sasebo-shi, Nagasaki Pref. Japan.
Email: mtamashima@fluidtechno.com, web: https://fluidtechno.com/

[*] Corresponding author: Tomoyo Nakayama, t-kaga@nakashima.co.jp

ABSTRACT

In this paper, we have shown the improvement of the overall performance of the hull of a 499 GT cargo ship, which has less flexibility in hull form design due to the Japanese domestic law. Most of the existing 499 GT cargo ships have V-type stern frame, which makes it difficult to obtain the effect of ducts, one of energy saving devices for ships. By shifting the cargo hold to afterward and adopting a stern form which is effective to install Nakashima Propeller' products "Neighbor duct", we aimed to improve the overall performance of a ship by making the bow finer. In a circulating water channel, we conducted a resistance, self-propulsion test and a wake measurement for a ship with a modified bulbous bow and a ship with and without a duct. As a result of the tests, it was confirmed that the forms of the bulbous bow were more effective in reducing the wave resistance and the duct enhances the propulsion performance. Especially, the useage of Nakashima Propeller' products GPX propeller improved the overall propulsion efficiency of the ship.

Keywords: hull form; propeller; energy saving device; CFD; circulating water channel; EEDI.

NOMENCLATURE

B_B	Maximum width at section X [m]
B_{mld}	Molded width of a ship [m]
C_b	Block coefficient [-]
C_{bB}	Block coefficient of bulbous bow [-]
d	The vertical distance from the water surface to the bottom of the under body of a ship [m]
D_B	Maximum height at section X [m]
D_{mld}	Molded depth of a ship [m]
F_n	Froude number [-]
H_{cbB}	The height of center of buoyancy of the bulbous bow [m]
L_B	The length from FP to the bulbous bow tip [m]
L_{pp}	Length between perpendiculars [m]
r_R	Residual resistance coefficient [-]
t	Thrust deduction fraction [-]
V	Ship speed [m/s]
V_x	Axial velocity [m/s]
V_r	Radial velocity [m/s]
V_θ	Circumferential velocity [m/s]
w_s	Wake fraction of full-scale ship [-]
Z_B	X's height of center of gravity [m]
γ_A	Run fullness coefficient [-]

γ_B Fullness of the bulbous bow [-]
γ_E Entrance fullness coefficient [-]
∇_B Displaced volume of bulbous bow [m^3]
η_H Hull efficiency [-]
η_R Relative rotative efficiency [-]
τ Definition of section form coefficient [-]

AP After Perpendicular
BHP Break Horse Power
CFD Computational Fluid Dynamics
EASM Explicit Algebraic Stress Model
EEDI Energy Efficiency Design Index
EEXI Energy Efficiency Existing Ship Index
EFD Experimental Fluid Dynamics
ESD Energy-Saving Device
FP Fore Perpendicular
GHG Greenhouse Gas
URANS Unsteady Reynolds-Averaged Navier-Stokes
X The mid position from FP to bulbous bow tip

1. INTRODUCTION

Improvement of propulsion performance of ships is required from the viewpoint of environmental problems and operational economy. EEDI, EEXI and zero emission efforts has been made mainly for large vessels. Furthermore, improvement of propulsion performance is required even for small vessels to which EEDI is not applied. For this purpose, synthesis optimization of the hull, propeller, rudder, and ESD is required. For small cargo ship, the calculation of gross tonnage is regulated by domestic law, which narrows flexibility in design. It makes improvement of propulsion performance difficult. Therefore, more and more overall hull form and performance optimization together with appendages such an ESD, should be made to contribute GHG matter. An optimization tool (AI method, etc.) can be useful, but an empirical method has been still used from convenience of treatment and reliability.

The stern of many domestic small cargo ships has a low resistance type so called V-type. It is known that a duct at the stern works more when the stern form has a larger longitudinal vortex which is apt to be generated by the stern, so called a U-type (Okamoto 2017). Since they have a V-type stern, the ducts are not effective and the hull form including energy-saving device has not been optimized.

The main objective in the present study is to propose the optimum small cargo ship with one of Nakashima Propeller' products "Neighbor duct" (Katayama 2017). The displacement at fore part is shifted to stern part installed the duct, keeping cargo hold space and gross tonnage in accordance with domestic low. Based on the Separability Principle of ship form (Taniguchi 1966) as the hull design element of small cargo ships, the influence of bow form, stern form, propeller, and energy-saving devices on propulsion performance is investigated.

2. CHARACTERISTICS OF SMALL CARGO SHIP AND DESIGN ELEMENTS

2.1 Characteristics of Small Cargo Ship

There is a need for the efficient ship that can carry a large amount of cargo on a ship with a small gross tonnage. For small cargo ships in Japan, the calculation of gross tonnage, determination of the main hull and the minimum number of crew members are specified in domestic law. The ships with small amount of gross tonnage are preferred because they require less crews. Actual results of past small cargo ships in Japan are shown in Figure 1. According to Figure 1, the ratio of ship length L_{pp} and ship width B_{mld} is often from 5.5

to 6.0. In addition, F_n at the design speed is higher than 0.22 and block coefficient C_b is more than 0.70. These tend to have higher F_n and larger C_b in the range of small vessels.

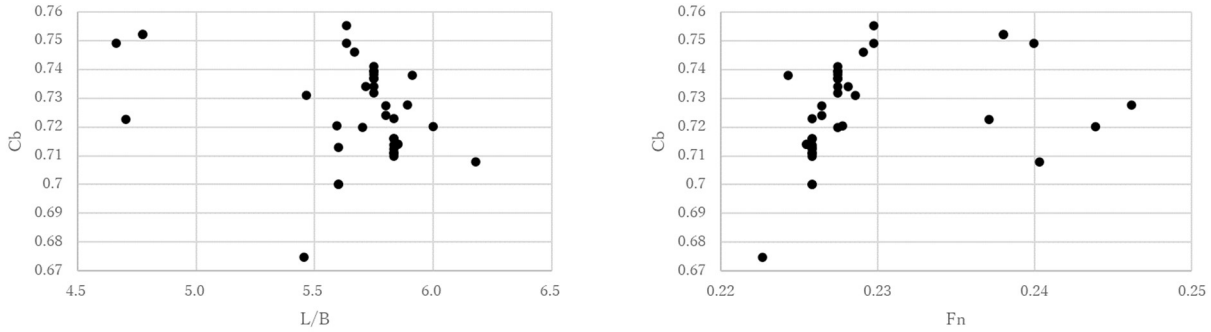

Figure 1. Main particulars.

2.2 Design Elements

2.2.1 Hull Form

A practical hull forms was designed with principal dimensions shown in Table 1. Figure 2 shows sectional area curves. The black line is a general sectional area curve of a conventional ship (The Coopetative Association of Japan Shipbuilders 1982). The red line is one of ship type proposed. Although the midship area is changed, the forebody of proposed hull is designed to be slenderer.

Table 1. The main hull objectives.

L_{pp}	B_{mld}	D_{mld}	d	C_B
71.00	11.50	7.12	4.13	0.73

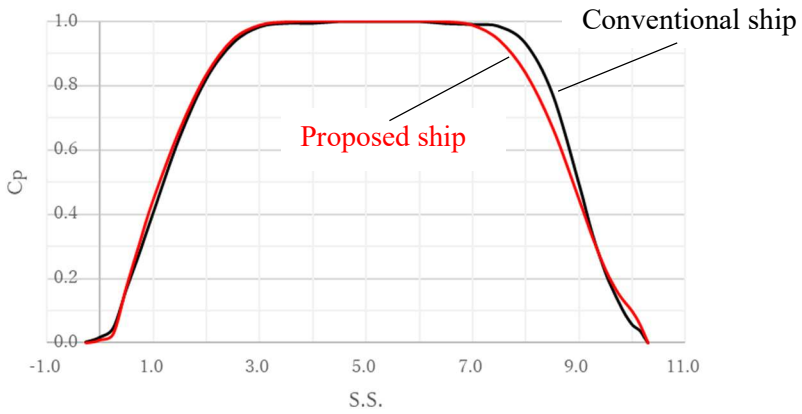

Figure 2. Sectional area curve.

Table 2. Entrance coefficient $\boldsymbol{\gamma_E}$ and run coefficient $\boldsymbol{\gamma_A}$.

	γ_E	γ_A
Conventional hull	0.537	0.432
Proposed hull	0.504	0.460

The entrance coefficient γ_E and the run coefficient γ_A for both hulls are shown on Table 2, which are defined as follows:

$$\gamma_E = \frac{B_{mld}/L_{pp}}{1.3(1-C_B)+0.031L_{CB}}, \tag{1}$$

$$\gamma_A = \frac{B_{mld}/L_{pp}}{1.3(1-C_B)-0.031L_{CB}}, \tag{2}$$

The fulless at the forebody of proposed hull is smaller and larger at the afterbody than those of conventional hull. The concept of proposed hull is to reduce wave generation at the front and to optimize the stern section containing the propellers and duct.

2.2.2 Bulbous Bow

The bulbous bows have three forms as shown in Figure 3. CFD simulation for the performance was made and model tests were conducted in a circulating water channel. When the length from FP to the bulbous bow tip is L_B, the mid position from FP to its tip is X. Further its maximum width at the section X is B_B, its height at the section X is D_B, and Z_B is the height of gravity at the section X, then the block coefficient of the bulbous bow is tentatively expressed as follows:

$$C_{bB} = \frac{\nabla_B}{L_B \times B_B \times d}, \tag{3}$$

The height of center of buoyancy H_{cbB} is expressed as follows:

$$H_{cbB} = Z_B - \frac{d}{2}, \tag{4}$$

The fullness of the bulbous bow is expressed with reference to the run coefficient as follows:

$$\gamma_B = \frac{B_B/L_B}{1.3(1-C_{bB})-0.031H_{cbB}}, \tag{5}$$

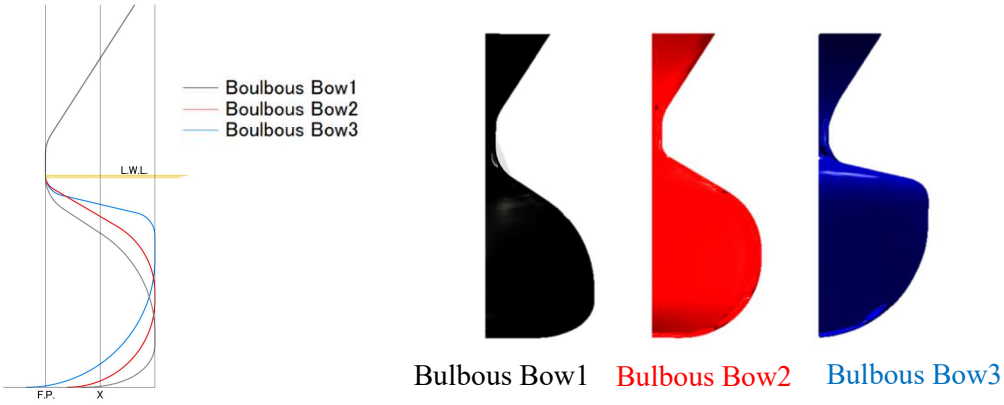

Figure 3. Bow configuration of bulbous bows.

The bulbous bows have three configurations as shown on Table 3.

Table 3. Fullness of the bulbous bow.

	γ_B
Bulbous Bow 1 (Black line)	1.45
Bulbous Bow 2 (Red line)	1.09
Bulbous Bow 3 (Blue line)	1.65

2.2.3 Stern Form

The black line shows the conventional stern form and the red line the proposed stern form in Figure 4.

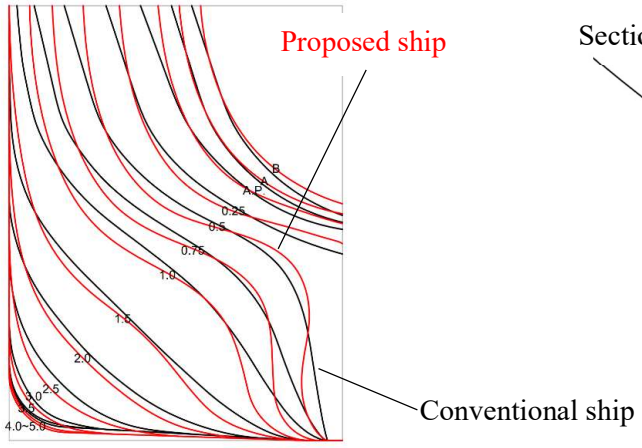

Figure 4. Afterbody section plan.

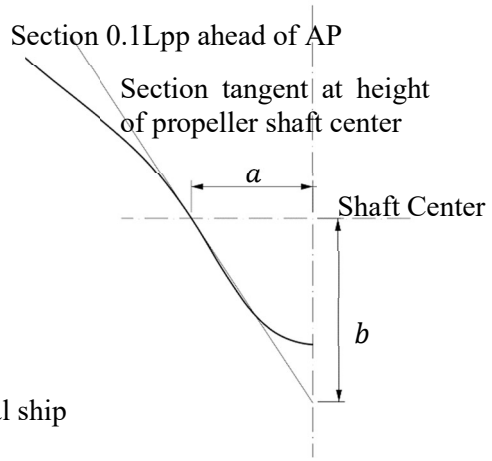

Figure 5. Stern frame definition.
(A Review of BSRA Work on Propeller Excited Vibration Project 1977)

If a and b are calculated with reference to Figure 5, τ is as follows:

$$\tau = \frac{a}{b}, \tag{4}$$

The both stern forms τ are shown on Table 4. Based on the respective values of τ, the conventional stern form is called Moderate V-Form and the proposed stern form is called Moderate U-Form.

Table 4. Definition of section form coefficient.

	τ
Conventional hull	0.692
Proposed hull	0.377

3. BULBOUS BOW AND WAVE MAKING RESISTANCE

3.1 Relationship between Model Test Conducted in a Circulating Water Channel and CFD

Model test and CFD simulation are performed for the different bulbous bows. The governing equations are the continuity equation and Unsteady Reynolds-averaged Navier-Stokes (URANS) equation. The artificial compressibility form of these equations based on a cell-centered finite-volume formulation is solved by structured grid-based solver, NAGISA developed at NMRI (Website at NMRI 2021) This tool is also used in the following paper (Hirata *et al.* 1999) (Ichinose *et al.* 2015) (Ichinose *et al.* 2017). The detailed conditions of CFD analysis are shown in Table 5.

Table 5. The detailed conditions of CFD analysis.

Governing equations	Continuity equation and URANS
Turbulence model	EASM
Discretization of space	Structured grid
Number of grids (half body)	161×81×81(double model) 161×105×81(free surface)
Solutions for Free Surface Calculation	Level set method

3.1.1 Accuracy of CFD

The wave pattern in the model test conducted in a circulating water channel is shown in Figure 6. The CFD result under the same condition as the model test is shown in Figure 7. Comparing these results, it can be confirmed that the wave profiles are almost equivalent to model test and CFD result.

Figure 6. Wave pattern in a circulating water channel ($F_n = 0.221$, Full condition).

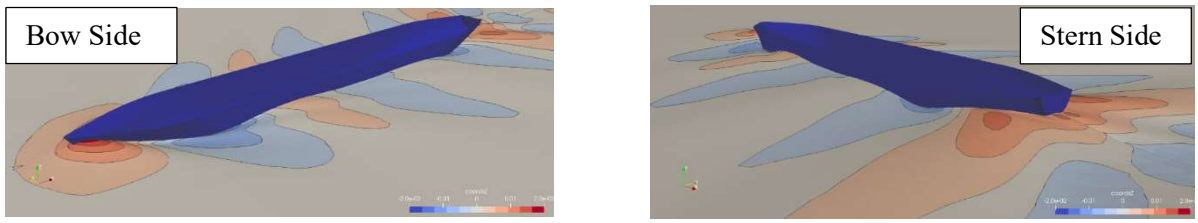

Figure 7. Wave pattern calculated by CFD ($F_n = 0.221$, Full condition).

3.1.2 Correlation between Model Tests and CFD

The model test of the conventional hull form has not been conducted. Therefore, the correlation r_R by CFD and model tests are obtained. This correlation is used to derive the equivalent r_R to the model test of conventional hull form. The correction between the model test and CFD is shown in Figure 8.

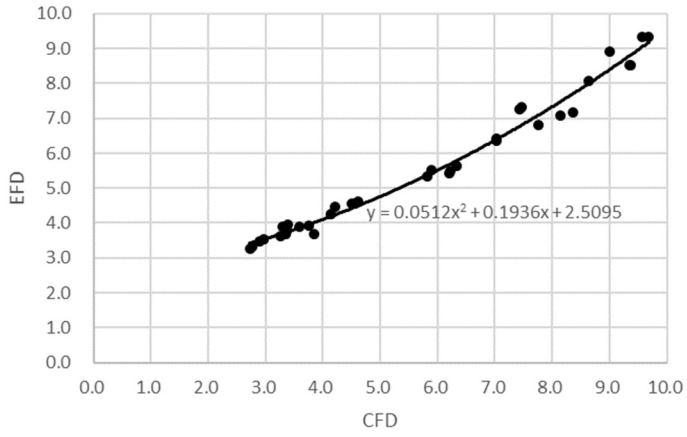

Figure 8. Correlation coefficient of r_R.

3.2 Comparison of r_R in Model Test

The model test is performed for the hull forms shown in Figure 3. The difference of Δr_R from the equivalent value to the model test of the conventional ship are shown for each form in Figure 9. Bulbous Bow 3 has the lowest ΔrR, whose profile has highest to closer the draft. However, the second lowest resistance is Bulbous Bow 1, indicating that resistance is not always lowered when the bulbous bow is close the draft. Figure 10 shows that the distance from the draft and volume of the bulbous bow have a major role in the reduction of resistance. The results show that a bulbous bow with a large volume close to the draft tends to be more effective in lowering the resistance, so the model test was conducted with the bulbous bow with a larger γ_B, and further improvement was obtained (yellow point in Figure 10).

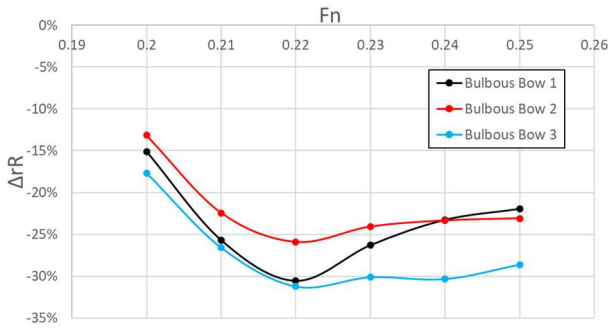

Figure 9. Results of the comparison of the difference Δr_R.

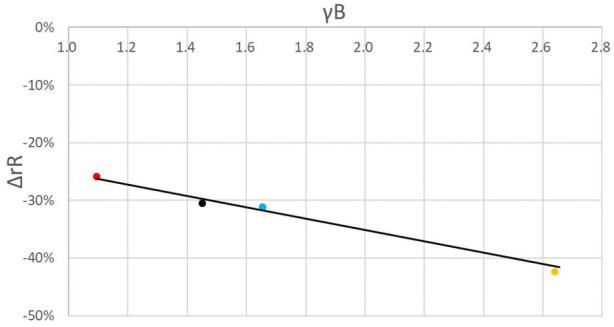

Figure 10. Relationship between Δr_R and bulbous bow fullness.

4. STERN FORM AND DUCT

4.1 Relation between Model Test and CFD

The detailed conditions of CFD analysis are shown in Table 6. In order to take into consideration, the influence of the duct attached at stern end. The overset grid is applied to discretize the space.

Table 6. The detailed conditions of CFD analysis.

Governing equations	Continuity equation and URANS
Turbulence model	EASM
Discretization of space	Structured grid and Overset grid
Number of grids (half body)	177×129×81(double model) 177×153×81(free surface) 81×65×73(rect grid) 69×161×41(duct grid)
Solutions for Free Surface Calculation	Level set method

Figures 11 and 12 show the wakefield measured in a circulating water channel. Each the line shows contour axial velocity. Figures 13, 14, and 15 show the wakefield calculated by CFD. From Figures 11 and 13 in case of no duct, the pattern of wake contour in the propeller disk shows a similar tendency. From Figures 12 and 14 in case of duct, the pattern of wake contour outside the duct in the propeller disk is similar. However, the flow in the duct by CFD is slower. This may be caused from the relatively large mesh around the ducts. As the ducts are relatively small to ship hull, so the mesh is coarse to fit the ship.

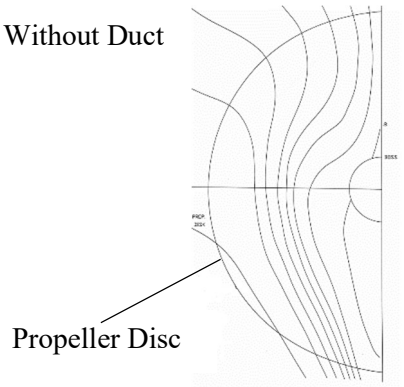

Figure 11. Wakefield of the proposed hull measured in a circulating water channel.

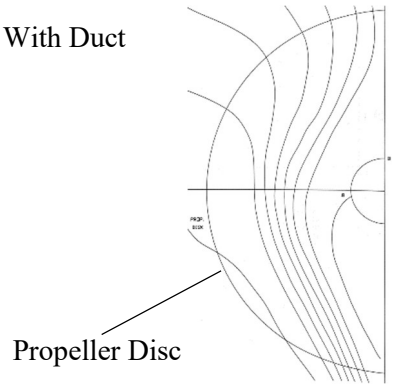

Figure 12. Wakefield of the proposed hull with duct measured in a circulating water channel.

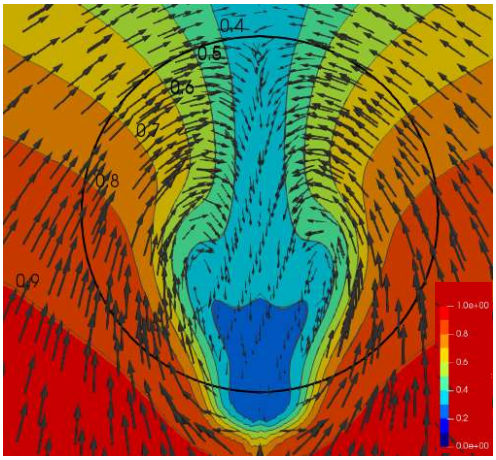

Figure 13. Wakefield of the proposed hull analyzed by CFD.

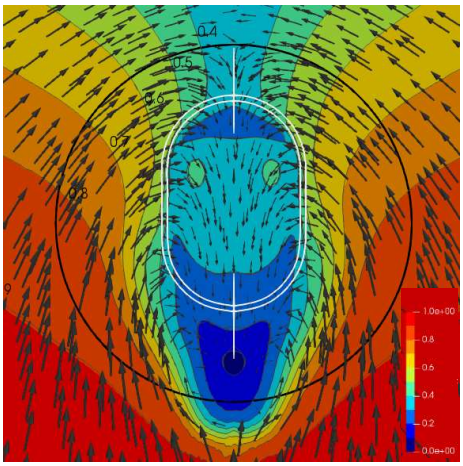

Figure 14. Wakefield of the proposed hull with duct analyzed by CFD.

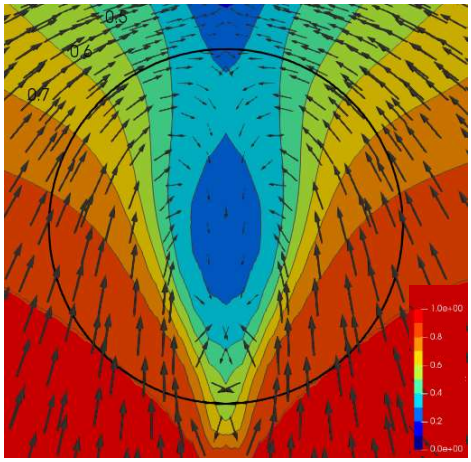

Figure 15. Wakefield of the conventional hull analyzed by CFD.

4.2 Effect of Stern Form and Duct on make distribution

4.2.1 Circumferential Distribution

The velocity distribution in the propeller disk shown in Figures 12, 13, and 14 is evaluated in terms of velocity components. Figure 16 shows the non-dimensionalized velocity distribution of the axial component in the

propeller disk for the conventional and the proposed hull with duct. The velocity distribution at the 0.7R position of the propeller shows that V_x/V of the proposed hull form is larger than that of the conventional hull form around the position of the propeller top. Therefore, the amount of propeller cavitation will be reduced. In addition, the proposed hull form has a slower slope in the range of 0 to 90 degrees where propeller cavitation occurs. Therefore, the risk of propeller cavitation erosion is expected to be lower in the proposed hull than in the conventional hull. The amount of cavitation and the risk of cavitation erosion are almost the same for the proposed hull in case of both no duct and duct, and the wake fraction in the propeller disk is reduced. Figure 17 shows the non-dimensionalized velocity distribution of the circumferential component in the propeller disk of the conventional and the proposed hull. The circumferential velocity distributions with larger amplitudes at the 0.3R and 0.7R suggest that the stronger longitudinal vortex is generated in the proposed hull than in the conventional hull.

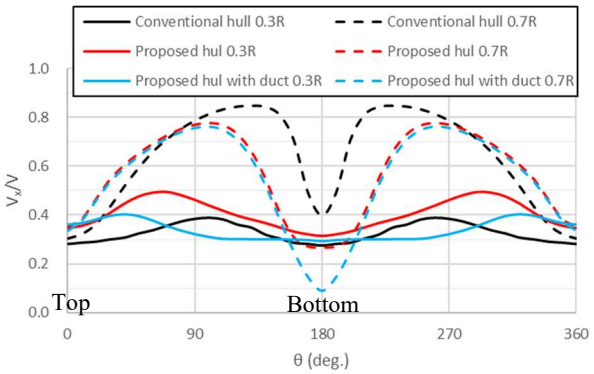

Figure 16. Circumferential distributions of axial velocity components by CFD.

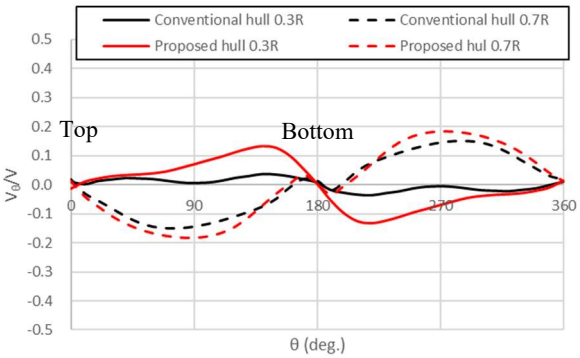

Figure 17. Circumferential distributions of circumferential velocity components by CFD.

Figure 18 shows the non-dimensionalized velocity distribution of the radial component at the leading edge of the duct of the conventional and the proposed hull. Around 270 to 90 degrees, it is thought that the duct of proposed hull generates more lift than that of the conventional hull. Because V_r/V is smaller and the attack angle of the flow into the duct is larger. Figure 19 shows the pressure distribution on the surface of duct. The pressure inside the duct is negative, therefore it can be assumed that the duct generated thrust.

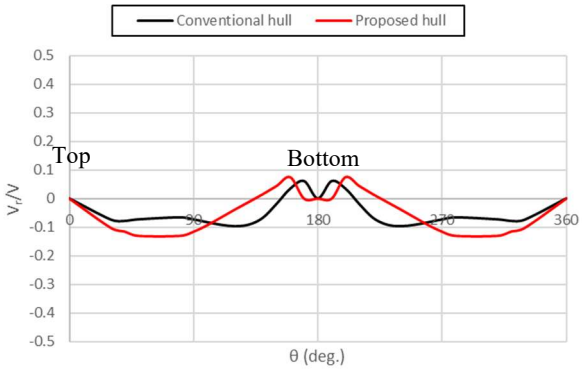

Figure 18. Circumferential distributions of radial velocity components by CFD.

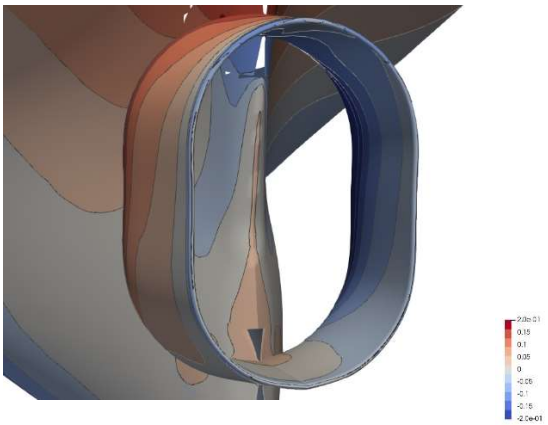

Figure 19. Pressure distribution on hull and duct surface by CFD.

4.2.2 Comparison of Self-Propulsion Factor of Model Test Equivalent

Table 7 shows the change of self-propulsion factor of the proposed hull based on the conventional hull. Since no model test is conducted for the conventional hull, the ratio of CFD results to the model tests of the proposed hull is taken as the equivalent model test result. Yazaki's diagram is used for wake fraction of full-scale ship (Yazaki 1969). The hull efficiency of the proposed hull with duct is increased by 1.7% compared to the conventional hull. The relative rotative efficiency is also increased by 1.0%.

Table 7. Variation of self-propulsion factor of proposed hull with duct from conventional hull.

$\Delta(1-w_s)$	$\Delta(1-t)$	$\Delta\eta_R$	$\Delta\eta_H$
-5.6%	-4.0%	1.0%	1.7%

5. PROPELLER

The propellers are designed using the results of model tests and equivalent model test. Figures 20 shows the conventional propeller. Figures 21 shows the GPX propeller. A conventional propeller which is 5% on Baril's chart is used for the conventional hull. GPX propeller can control the disappearance of cavitation even if the amount of cavitation increases, and the tip rake can reduce the fluctuating pressure. The main particulars of the both propellers are shown in Table 8. The propeller open water efficiency of GPX propeller is increased by 2% compared to the conventional propeller.

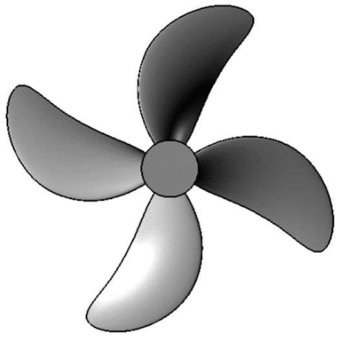

Figure 20. The geometry of the conventional propeller.

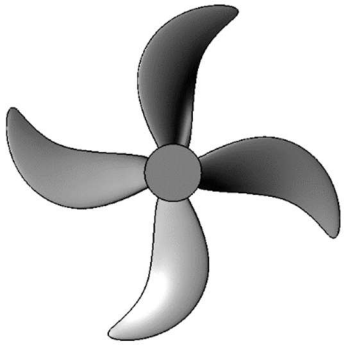

Figure 21. The geometry of GPX propeller.

Table 8. Propeller main particulars.

	The conventional propeller	GPX propeller
Number of blades	4	4
Diameter [m]	2.7	2.7
Pitch ratio (0.7R)	0.675	0.684
Expanded area ratio	0.44	0.34

6. CONCLUSIONS

As a result of synthesis optimization of the hull, propeller and energy-saving devices, the proposed hull with duct was able to reduce BHP by 33% compared to the conventional hull. The details of the efficiency increase

are 29% for ships, 2% for ducts, and 2% for propellers. Since the hull was designed equipped with ducts, the forebody of the hull could be made slender, which significantly reduced the wave making resistance. The bulbous bow was found to have a significant effect on the wave making resistance, not only because of the submerged distance from the water surface, but also because of the volume of the bulbous bow.

ACKNOWLEDGEMENTS

I am grateful to K. Mokuo of Fluid Techno Co., Ltd. for cooperation in the hull form design, M. Hirota of Shipbuilding Research Centre of Japan for cooperation in the CFD calculation and K. Tanaka of West Japan Fluid Engineering Laboratory Co., Ltd. for cooperation in the model test conduct.

REFERENCES

A Review of BSRA Work on Propeller Excited Vibration Project. (1977). *The British Ship Research Association*

Hirata, N. and Hino, T. (1999). An Efficient Algorithm for Simulating Free-surface Turbulent Flows around an Advancing Ship. *Journal of The Society of Naval Architects of Japan*, vol.185, pp.1-8

Ichinose, Y., Kume, K. and Tahara, Y. (2017). A Construction and Evalution of Hull-form Database for Domestic Vessels with Regulation on Gross Tonnage - Development of a Prototype for 749GT-type Domestic General Cargos -. *Journal of the Japan Society of Naval Architects and Ocean Engineers*, vol.56, pp.51-62

Ichinose, Y., Tahara, Y. and Kasahara, Y. (2015). Numerical on Flow Field around the Aft Part of Hull Form Series in a Steady Flow. *Nutts*

Katayama, K., et.al. (2017). Propulsion Performance Optimization of "Neighbor Duct" by CFD. *Proceedings of MARINE 2017*, pp.529-537.

Okamoto, N., Suzuki, K., Takanori, H. and Masuda, S. (2017). An Optimization Method of Stern Hull Form to Minimize Brake Horse Power (2nd Report) - Optimization of Hull Form with Super Stream Duct as Energy Saving Device -. *Journal of the Japan Society of Naval Architects and Ocean Engineers*, vol.26, pp.27-34.

Taniguchi, K., Watanabe, K. and Tamura, K. (1966). On a New Method of designing Hull Form of Large Full Ship based on the Separability Principle of Ship Form. *Zosen kyokai syuuki kouennkai*

The Coopetative Association of Japan Shipbuilders. (1982). *Technical Guidance for Designing Energy-saving small vessels (499 gross tonnage cargo ship).* pp.91~92, (1982)

Web site: National Maritime Research Institute, https://www.nmri.go.jp/study/research_organization/fluid_performance/cfd/group2_1, (accessed on 29th April 2021).

Yamasaki, S., Okazaki, A., Katayama, K., Himei, K., Mishima, T. and Hasuike, N. (2010). High Efficiency Propellers-NHV (Non Hub-Vortex) Propeller with Smallest Blade Area. *IPS'10 International Propulsion Symposium*

Yazaki, A. (1969). A Chart for Estimating Wake Fraction of Actual Ships from Tank Test Results by using Model Ships. *Bulletin of the Society of Naval Architects of Japan*, Vol. 40, pp.270-272.